Imperial College London

EGU2020: Sharing Geoscience Online
5th May 2020

Timescales of Ionospheric Field-Aligned Currents during a Geomagnetic Storm: Global Magnetospheric Simulations

Joseph Eggington[1]

J. C. Coxon[2], R. M. Shore[3], J. P. Eastwood[1], L. Mejnertsen[1], R. T. Desai[1], J. P. Chittenden[1]

[1] Blackett Laboratory, Imperial College London, London, United Kingdom
[2] Space Environment Physics Group, University of Southampton, Southampton, United Kingdom
[3] British Antarctic Survey, Cambridge, United Kingdom

j.eggington17@imperial.ac.uk

Science & Technology Facilities Council

Outline

1. Introduction
2. Simulating a Geomagnetic Storm
3. Global Stormtime Dynamics
4. Ionospheric Response Timescales
5. Conclusions + Future work

Introduction

- Geomagnetic storms generate a complex and highly time-dependent response in the magnetosphere-ionosphere system
- FAC signatures can be very localised, with timescales of response across the polar cap varying with respect to different IMF components (e.g. Anderson + 2017 SpW, Browett + 2017 JGR)
- Global MHD simulations provide means to globally model magnetospheric and ionospheric conditions during a real event, allowing direct comparison to space- and ground-based observations
- **This study:**
  - We perform global simulations of a real geomagnetic storm, comparing to observations using FAC data from AMPERE and ground magnetic field data from SuperMAG
  - From this we place the observations global context to better understand the physical drivers behind the system's response, and the magnetospheric dynamics associated with the key timescales

Calculating Ionospheric Response Timescales

- In this study we use an approach based on the Spatial Information from Distributed Exogenous Regression (SPIDER) technique, first applied to ground magnetic field data from SuperMAG (Shore + 2019 JGR) and later adopted to analyse AMPERE data (Coxon + 2019 JGR)

- In this method a gridded quantity (e.g. FAC) on ionosphere/ground is cross-correlated with time-lagged solar wind parameters (e.g. IMF B_Z)

- The timelag that generates the strongest correlation represents the most characteristic response timescale to the given solar wind parameter at that particular grid point

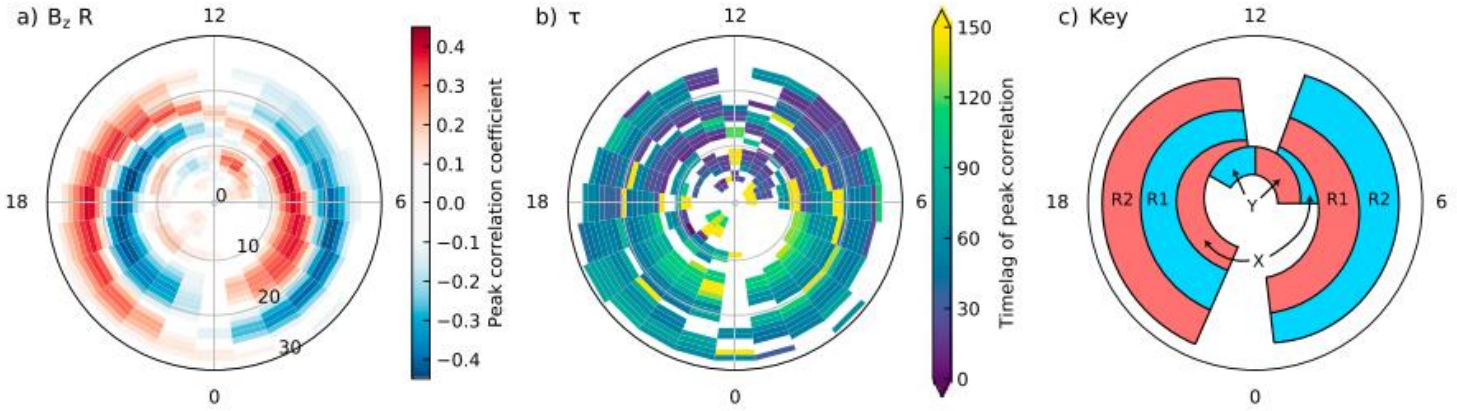

Figure 1 – The above technique as applied to AMPERE data covering the month of March 2010, taken from Coxon et al. (2019). The correlation profile in the left panel reveals the underlying ionospheric current systems (right), with the corresponding timescales (centre).

Selecting a Geomagnetic Storm

- Storm selected from list in Murphy + 2018 GRL (supp. info)
- Chose storm 34, lasting from 3rd – 7th May 2014: preceding period of fairly steady, quiet SW conditions, ideal to initialise magnetosphere
- Strongest FAC seen during first 20h of storm (highlighted) – we choose this period to simulate
- Good coverage of AMPERE and SuperMAG data over storm duration

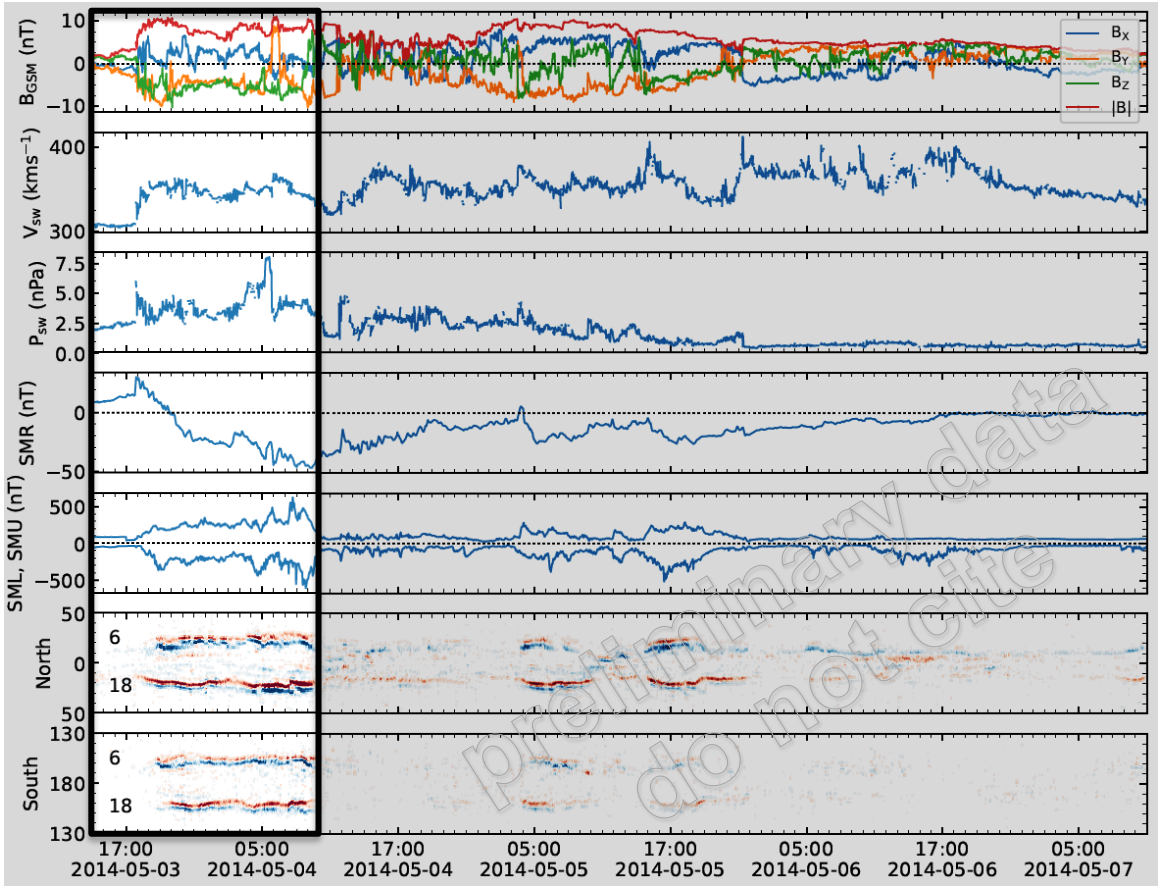

Figure 2 – Geomagnetic storm data for the chosen event, with keograms of FAC data from AMPERE shown in the bottom 2 panels (Credit: J. Coxon)

The Gorgon MHD Code - Overview

- Fully explicit, Eulerian formation of the resistive MHD equations on a uniform 3D Cartesian grid (Ciardi + 2007 Phys. Plas.)
- Satisfies $\nabla \cdot \vec{B} = 0$ to machine precision via vector potential and staggered grid
- Used to model Neptune's magnetosphere and outer boundaries of Earth's magnetosphere (Mejnertsen + 2016 JGR, 2018 JGR)
- Thin-shell ionosphere model captures magnetosphere-ionosphere coupling as inner boundary condition (Eggington + 2018 A&G)

$$\frac{\partial \rho}{\partial t} + \nabla \cdot (\rho \mathbf{v}) = 0$$

$$\frac{\partial}{\partial t}(\rho \mathbf{v}) + (\mathbf{v} \cdot \nabla)\rho \mathbf{v} = -\nabla \left(P_{\mathrm{p}} + P_{\mathrm{e}}\right) + \mathbf{J} \times \mathbf{B}$$

$$\frac{\partial \epsilon_{\mathrm{p}}}{\partial t} + \nabla \cdot \left(\epsilon_{\mathrm{p}} \mathbf{v}\right) = -P_{\mathrm{p}} \nabla \cdot \mathbf{v} - \Delta_{\mathrm{pe}}$$

$$\frac{\partial \epsilon_{\mathrm{e}}}{\partial t} + \nabla \cdot \left(\epsilon_{\mathrm{e}} \mathbf{v}\right) = -P_{\mathrm{e}} \nabla \cdot \mathbf{v} + \eta |\mathbf{J}|^2 - \Lambda + \Delta_{\mathrm{pe}}$$

$$\frac{\partial^2 \mathbf{A}}{\partial t^2} = -c^2 \nabla \times \nabla \times \mathbf{A} + \frac{\mathbf{J}}{\epsilon_0}$$

$$\text{where} \quad \eta \mathbf{J} = -\frac{\partial \mathbf{A}}{\partial t} + \mathbf{v} \times \mathbf{B}$$

ρ: *Mass Density*	$\mathbf{A}$: *Vector potential*
$\mathbf{v}$: *Velocity*	$\mathbf{B}$: *Magnetic field*
$P_{p,e}$: *Pressure*	$\mathbf{J}$: *Current density*
$\epsilon_{p,e}$: *Energy Density*	η: *Resistivity*
Δ_{pe}: *Electron-ion energy exchange*	
Λ: *Optically thin radiation losses*	

Simulation Set-up

- Simulated for 20h driving with upstream solar wind data from ACE
  - Magnetosphere initialised after ~2h, focus on conditions for t > 2h
- Dipole tilt and rotation captured through use of Solar-Magnetic (SM) coordinates

Simulation parameters

- Solar wind
  Upstream data from ACE over duration of storm (N.B. setting B_x = 0)
- Domain
  X = [-30, 90] R_E, Y = [-40, 40] R_E, Z = [-60, 60] R_E, 0.5 R_E grid res.
- Field
  Dipole M = 7.94e22 Am^{-2} at origin, aligned with SM Z-axis
- Ionosphere
  Non-uniform conductance captures EUV ionisation (Moen and Brekke 1993 GRL), using $F_{10.7}$ = 100, with a floor value of $\Sigma_{P,H}$ = 3 mho

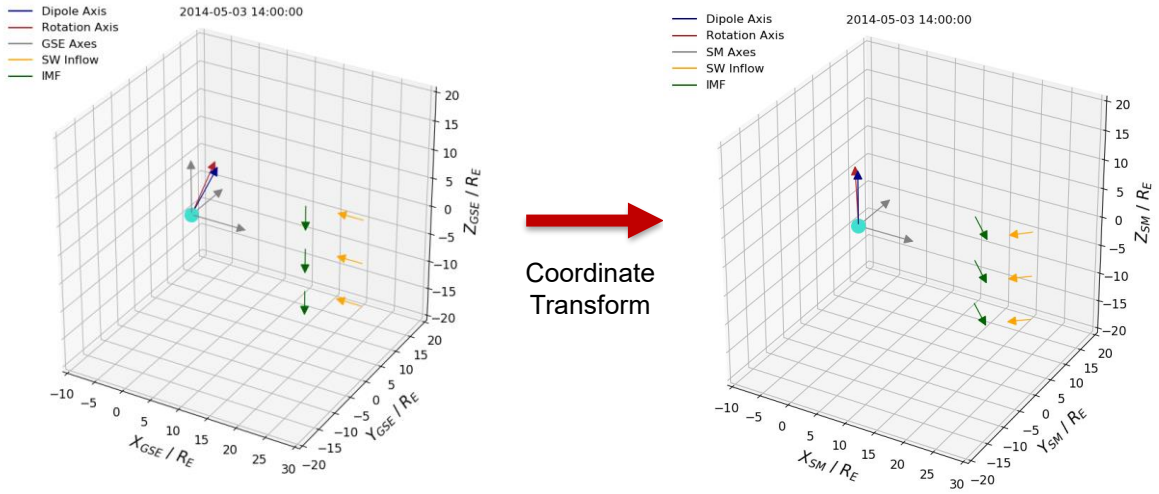

Figure 3 – Coordinate transform from GSE (Geocentric-Solar-Ecliptic) to SM, showing how the motion of the dipole axis is projected onto the solar wind input

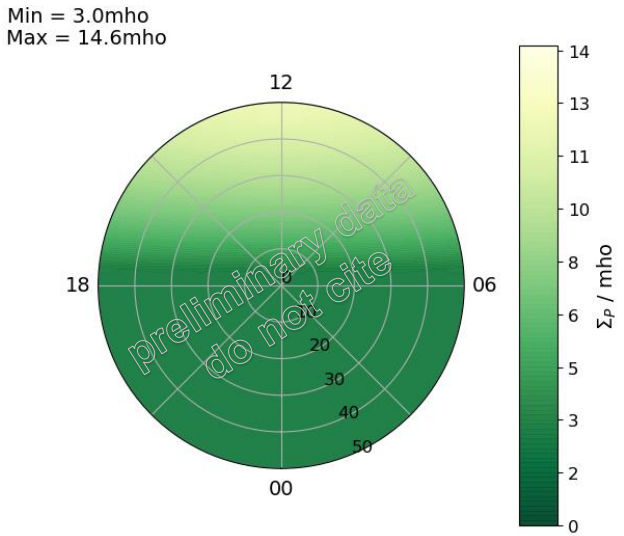

Figure 4 – Conductance profile used in the simulation, showing Pedersen conductance

Selecting a Geomagnetic Storm – Simulation Input

- Southward IMF turning and dynamic pressure spike occurs ~3h (17:00 UT)
- IMF mostly southward for following day, turning northward after ~18h
- We initialise the magnetosphere using the first ~3h of data, and simulate the following 17h of the storm
- We analyse the magnetospheric and ionospheric response over this period

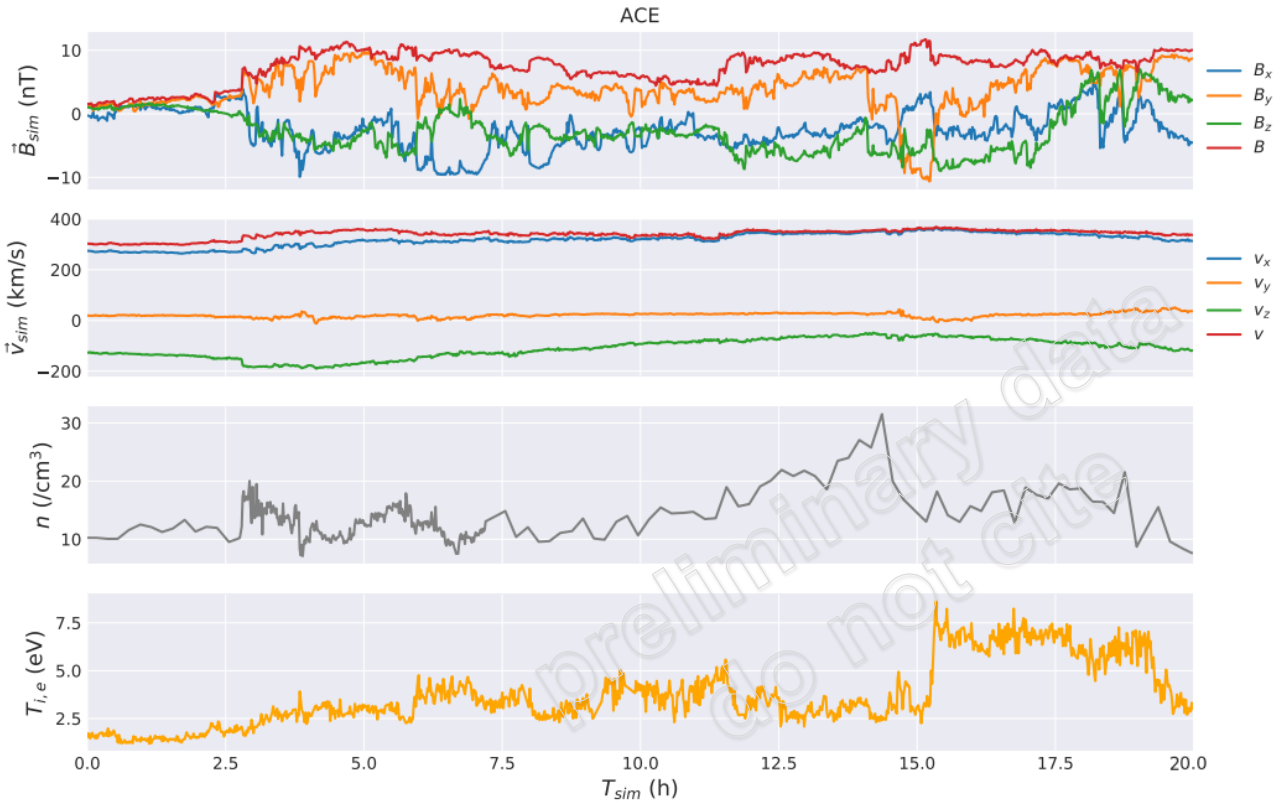

Figure 5 – Solar wind conditions used to drive the simulation, taken from ACE data and rotated into simulation coordinates (X,Y,Z) = ($-X_{SM}$,$-Y_{SM}$,Z_{SM}). Note 0h corresponds to 14:00 UT on 2014-05-03

Storm Overview – Dayside Reconnection Rate

- Traced 3-D reconnection X-line (magnetic separator) on magnetopause during storm by identifying magnetic topology on dayside (Figure 2), based on method of Komar + 2013 JGR
- Repeated in intervals of 10 minutes and calculated dayside reconnection rate $V_{rec} = \int \vec{E}_{||} \cdot d\hat{l}$ along separator, where $\vec{E}_{||}$ is parallel to the X-line.
- V_{rec} increases from 2h-6h, dropping for next ~2h as IMF B_z becomes less negative
- Increases again for following 10h, reaching a peak between 14h-15h

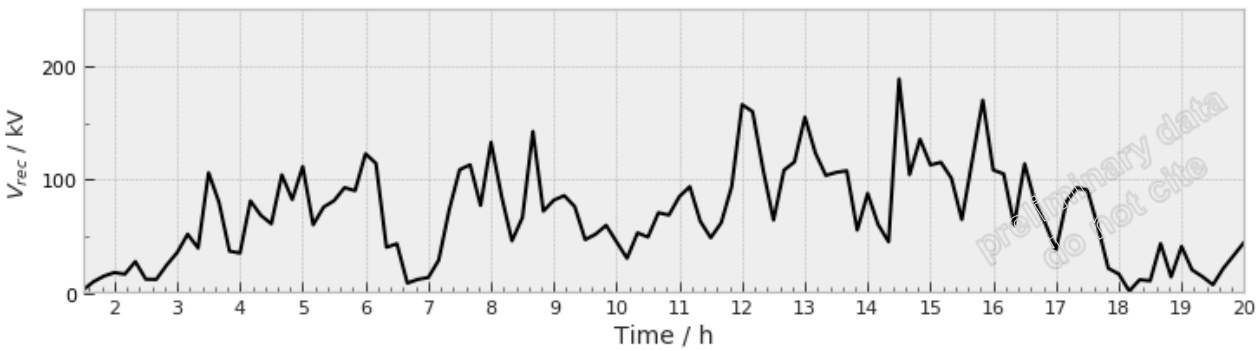

Figure 6 – Dayside reconnection voltage calculated over the duration of the simulation

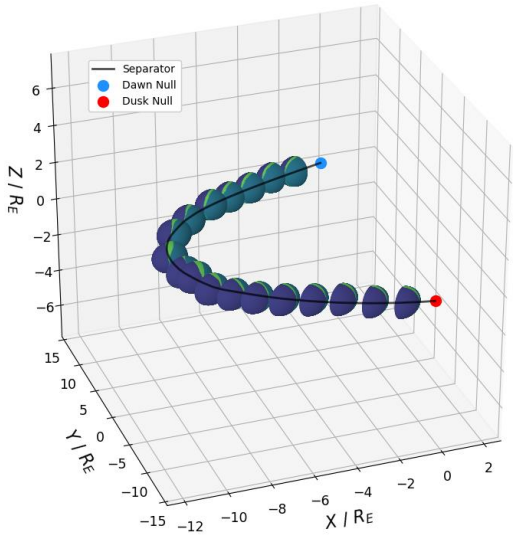

Figure 7 – Technique used to trace separator, iteratively locating convergence points of magnetic domains on magnetopause (taken from Eggington + 2020 JGR, in review)

Storm Overview – Polar Cap Size

- Polar cap expands by ~10° latitude from 2h-5h and contracts from 18h-20h; motion of region-I FAC as per the expanding-contracting polar cap (ECPC) paradigm leads to 'banding' in timelag maps (Fig. 13)

- Slight day-night and dawn-dusk asymmetry in average OCB location in each hemisphere, with largest variation in post-noon sector – asymmetries may be due to dipole tilt variation or influence of B_y

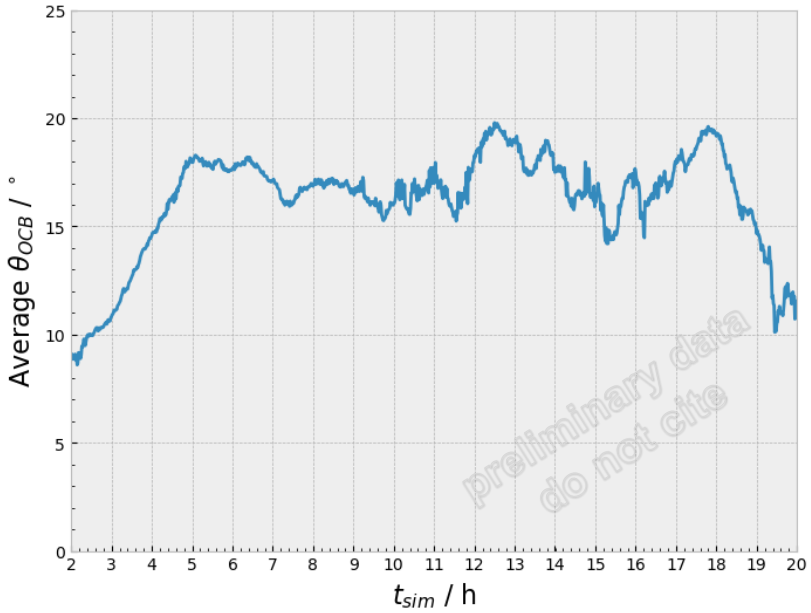

Figure 8 – Average stormtime latitude of the open-closed boundary (OCB) in the northern hemisphere

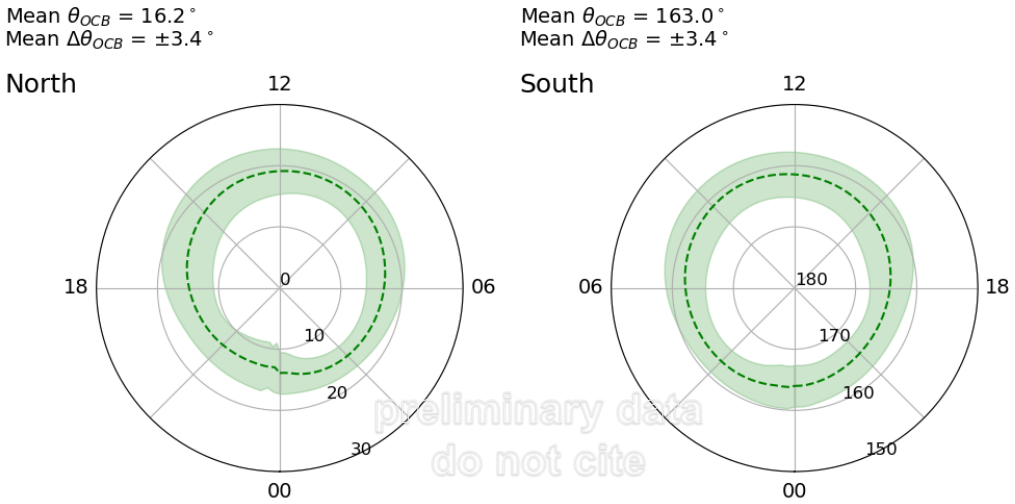

Figure 9 – Average location of the open-closed boundary (OCB). The green shaded region represents one standard deviation during the simulation

Storm Overview - Ionospheric Response

- Slight delay (~30min) between initial change in OCB and response of ionosphere
- Sharp rise in CPCP and TFAC from 3h-6h, dropping due to reduced reconnection rate (Fig. 8) before rising again
- Region-I FAC migrates to lower latitudes with OCB after ~3h
- Most intense FAC from 10h-18h, but takes ~2h to weaken and return to low latitudes following northward IMF turning
- Suggests longer timescales for nightside reconnection to occur, slowing response at start and end of simulated period

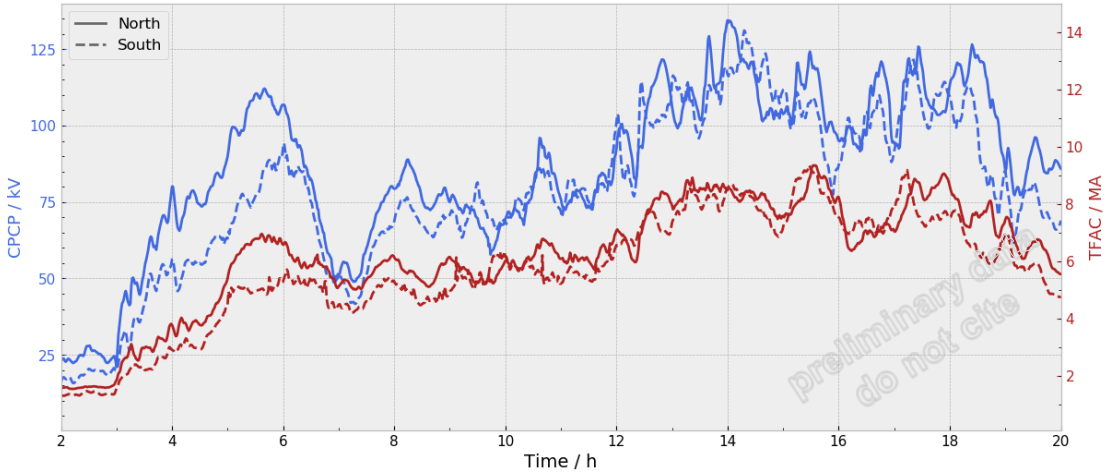

Figure 10 – Total field-aligned current (TFAC) and cross-polar cap potential (CPCP) on the ionosphere over the duration of the simulation

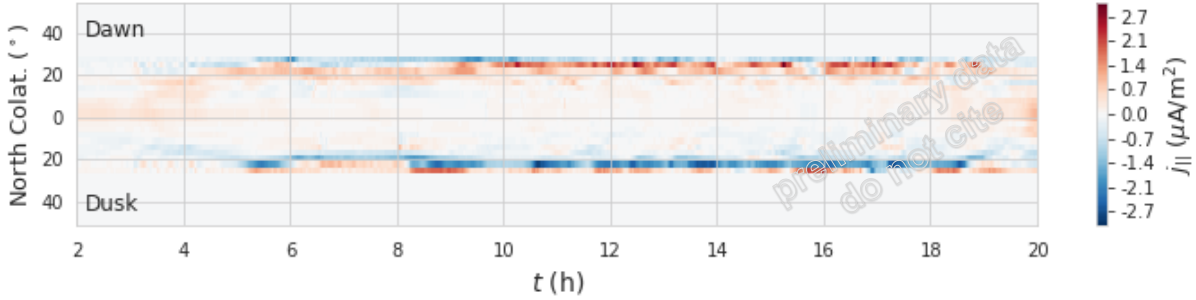

Figure 11 – Keogram of northern ionospheric FAC taken through the dawn-dusk meridian

Storm Response Timescales – AMPERE Data

- Peak correlations and timelags for IMF B_y and B_z, data covers whole 5 days of storm
- R-I current visible in B_z correlation patterns, with banding in timescales occurring over range of ~10˚ latitude
  - Consistent with simulated OCB locations
  - Long timelags on nightside of polar cap – slow response of nightside reconnection and migration of FAC?
- Timescales for B_y longest at midnight-to-dawn sector, where we see least variation in OCB; asymmetry may be related to B_y influence on tail
- Next step: producing same plots from simulated FAC for more direct comparison

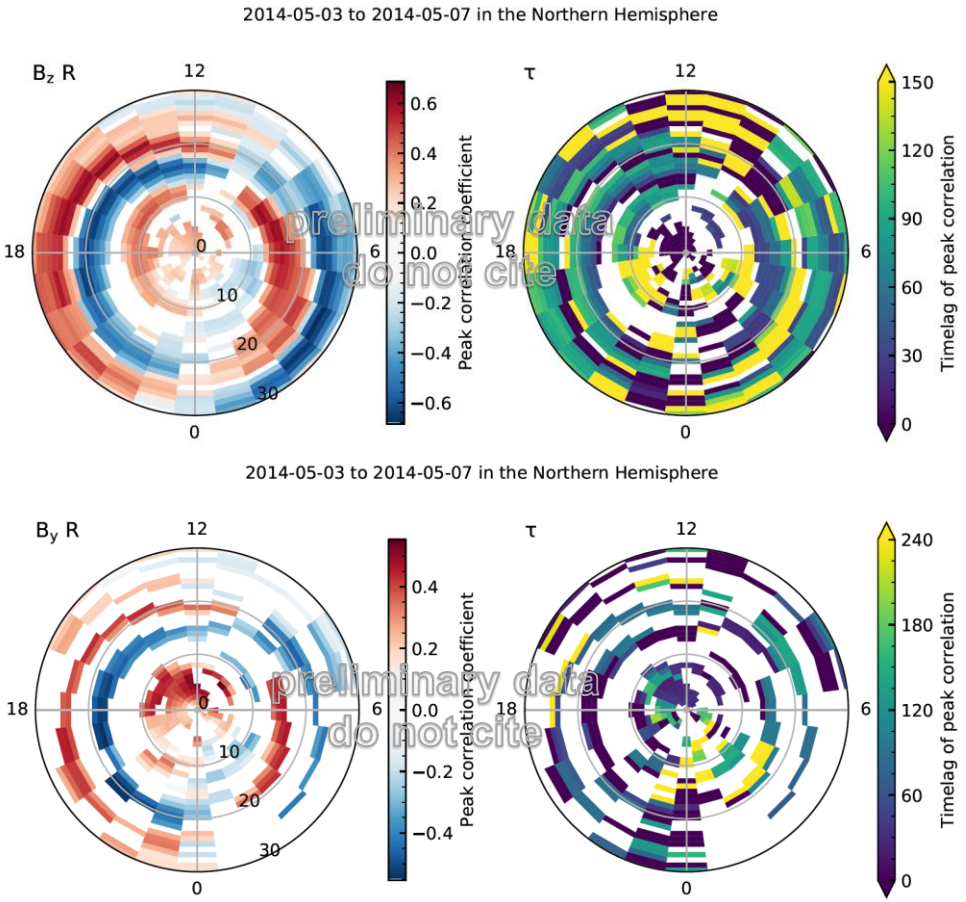

Figure 12 – Results from AMPERE data showing peak correlation coefficients (left) and associated timelags (right) for IMF B_z (top) and B_y (bottom) (Credit: J. Coxon)

Storm Response Timescales – SuperMAG Data

- Peak correlations and timelags for IMF B_y and B_z, data covers whole 5 days of storm
- Outputs from surface external and induced magnetic field (SEIMF) model (Shore + 2018 JGR) based on SuperMAG data
  - As before, longer B_z timescales on nightside at high latitudes, but B_y timelags generally shorter
  - Further analysis of simulation data needed for direct comparison

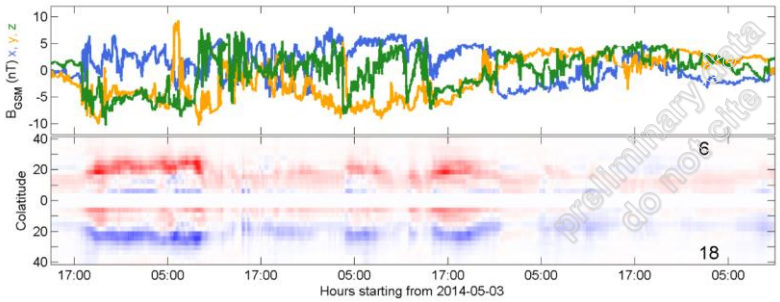

Figure 13 – Keogram of SuperMAG data during the storm, showing the southward ground magnetic perturbation (Credit: R. Shore)

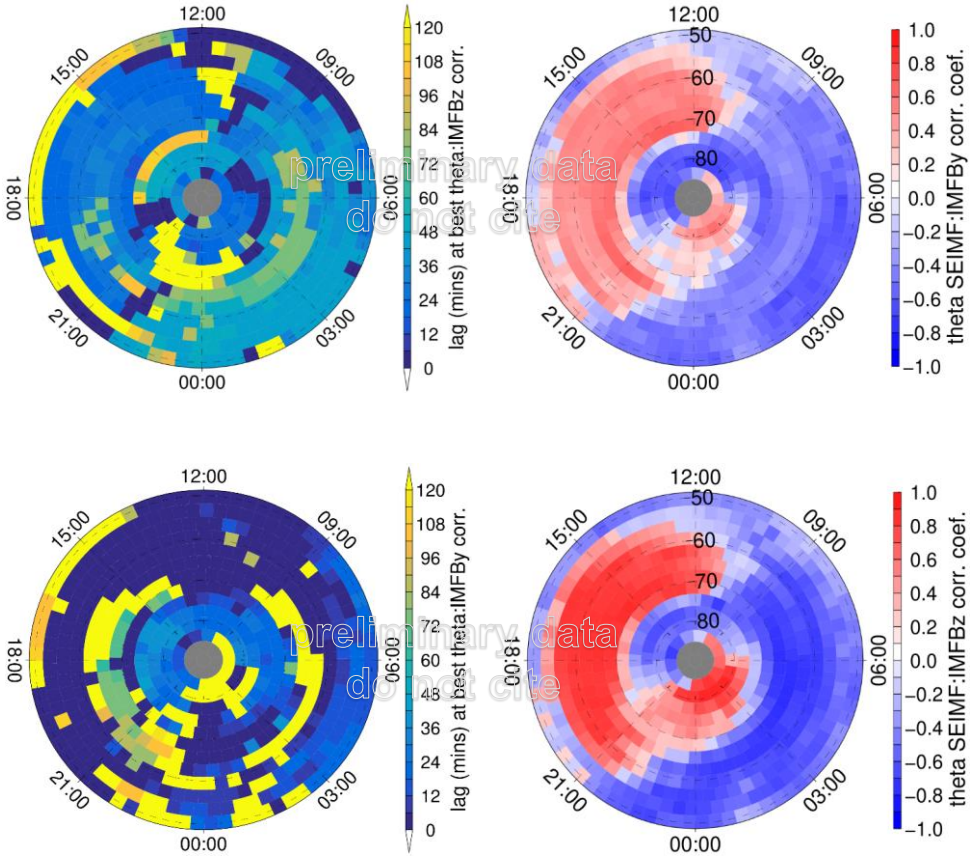

Figure 14 – Results from SuperMAG data showing peak correlation coefficients (left) and associated timelags (right) for IMF B_z (top) and B_y (bottom) (Credit: R. Shore)

Conclusions

- The simulation captures in detail the expansion and contraction of the polar cap during the storm, and the changes in reconnection rate that drive the resulting enhancement and migration of the FAC
- Agreements are found with the observed timelag patterns in AMPERE data, such as extent of banding due to the region-I currents and existence of asymmetries between day-night and dawn-dusk
- **Next steps:**
  - Simulate with a less simplistic conductance by including electron precipitation in auroral region
  - Compute correlation and timelag maps using simulated ionospheric FAC data for direct data-model comparison
    - Similarly, can use simulated FAC to generate time-series of ground magnetic field to compare to SuperMAG data
    - Can also cross-correlate with simulated parameters like reconnection rate as well as IMF – this can help identify which parameters are most relevant to the stormtime response
  - Simulate different phases of the storm to determine how the response timescales evolve, rather than focusing on a single peak correlation

This work was funded by STFC (grant ref. ST/R504816/1) and NERC (SWIGS and RadSat projects), and used the Imperial College High Performance Computing Service (doi: 10.14469/hpc/2232).

Science & Technology Facilities Council